submitted to *The Astrophysical Journal Letters*

Detection of the Angular Correlation of Faint X-ray Sources

A. Vikhlinin[1]
Space Research Institute, Profsoyuznaya 84/32,Moscow 117810, Russia.
vikhlinin@hea.iki.rssi.ru

and

W. Forman
Harvard-Smithsonian Center for Astrophysics, 60 Garden street, Cambridge, MA 02138, USA.
wforman@cfa.harvard.edu

ABSTRACT

We have analyzed a set of deep ROSAT observations with a total sky coverage of 40 square degrees to search for clustering of faint X-ray sources. Using the resulting catalog of discrete X-ray sources, we detect, for the first time in X-rays, a positive correlation on angular scales of $0\farcm5$–$10'$. When corrected for a bias due to limited spatial resolution which amplifies the correlation, the observed angular correlation function agrees well with that expected from the spatial correlation of optically selected quasars, provided that they comprise an appreciable fraction ($\geq 50\%$) of detected X-ray sources.

Subject headings: cosmology: observations – quasars: general – X-rays: galaxies

[1]Visiting CfA

1. INTRODUCTION

Models of the X-ray background composition can be strongly constrained by the study of its arcminute-scale fluctuations. For example, Soltan & Hasinger (1994, hereafter SH94) have shown that a highly correlated population of point sources cannot produce more than 35% of the still unresolved fraction of the X-ray background. Until now the angular correlation of X-ray sources has not directly been measured, and the usual approach in X-ray studies is to assume a spatial correlation model for X-ray sources inferred from optical observations. In this *Letter* we report the first detection of a positive angular correlation of X-ray sources detected in a set of medium-deep exposure ROSAT fields covering a total area of 40 square degrees. The correlation is detected on both small ($\lesssim 1'$) and moderate ($1'$–$10'$) angular scales.

This work continues our series of papers (Vikhlinin et al. 1995a,b,c, hereafter Papers I, II, III) in which we developed an efficient method for detection of point sources (Matched Filter, Paper I), and applied it to a set of 130 long exposure high Galactic latitude ROSAT/PSPC images. Papers II and III discuss the number-flux relation and average spectra of faint X-ray sources. In the present study, we explore the spatial distribution of X-ray sources by means of the two-point angular correlation function. We show that the detected angular correlation is consistent with that expected if X-ray sources are distributed in space like optically selected quasars. We compare our results to the angular correlation of the fluctuations in the X-ray background (e.g., Georgantopoulos et al. 1993 and SH94).

2. DATA AND ANALYSIS

Our sample consists of 254 medium and deep exposure ROSAT observations all having high Galactic latitudes ($|b| > 30^\circ$) and low galactic absorption ($N_{\rm H} < 6 \times 10^{20}$ cm^{-2}). When possible, we stacked several ROSAT pointings in the same direction, thus increasing the exposure for several fields. The data were screened for high particle and solar scattered background periods (Snowden et al. 1994). Special precautions were taken to exclude intervals of bad satellite aspect. The exposure times range from $\sim 5,000$ s to $\sim 100,000$ s, with minimum detectable fluxes from $\sim 5 \times 10^{-14}$ ergs s^{-1} cm^{-2} to $\sim 1.2 \times 10^{-15}$ ergs s^{-1} cm^{-2} for the shortest and longest exposure fields, respectively. The effective sky coverage is 40 square degrees at bright fluxes, begins to decrease below 5×10^{-14} ergs s^{-1} cm^{-2}, and remains significant down to at least $\sim 4 \times 10^{-15}$ ergs s^{-1} cm^{-2}, where the coverage is 1 square degree.

Compared to our previous study of the X-ray number-flux relation and average source spectra (Papers II, III), we have doubled the geometrical sky coverage, predominantly by

inclusion of a large number of lower exposure fields. On the other hand, any pointing which had a normal galaxy as its target, which could potentially contaminate the sample by inclusion of highly correlated and/or extended sources related to those galaxies, has been excluded. For the purposes of the present analysis, we used only the central parts ($< 12'$ off-axis) of ROSAT images, excluding also a $3'$ radius circle around the targets of observations. Data analysis was performed in exactly the same way as described in Papers I and II.

The conventional way to determine the two-point angular correlation function (ACF) is to calculate the ratio of the number of pairs of sources in the real data (DD), which fall in the separation range of $(\theta, \theta + d\theta)$, and the number of those pairs expected when the spatial distribution of sources is random (RR): $\hat{w}(\theta) = \frac{DD}{RR} - 1$. Since the source detection efficiency decreases far off the telescope axis (primarily because of the PSF degradation), the appropriate way to determine RR is to simulate observations with the background and the source number-flux relation found in actual observations, apply the detection algorithm to the simulated images, and compute RR as the number of detected source pairs found in the simulated data.

Simulations were performed according to the following procedure. The source positions were chosen uniformly at random. Source fluxes were then determined from the log N - log S distribution measured in Paper II ($N(> S) \propto S^{-1.55}$ for $S > 2.2 \times 10^{-14}$ ergs s^{-1} cm^{-2} and $N(> S) \propto S^{-0.86}$ below this flux). The differential log N - log S was truncated at a limiting flux, $f_{\rm min} = 3 \times 10^{-18}$ ergs s^{-1} cm^{-2}, which is almost three orders of magnitude below the detection threshold of the deepest observation, and corresponds to a source surface density of ~ 10 per PSF circle. At the limiting flux value, the number of photons per source is much less than 1, so that the contribution from sources below $f_{\rm min}$ is indistinguishable from truly diffuse emission. Source fluxes were converted to counts (after accounting for the telescope vignetting function) using the counts-to-flux conversion coefficient calculated for an absorbed $\alpha = 1$ power-law spectrum, with the absorption fixed at the appropriate Galactic value for each ROSAT observation. The number of source photons was drawn from a Poisson distribution. Photons were distributed over the images according to the PSF approximation of Hasinger et al. (1993).

To achieve the requirement of having the same background in the real and simulated data, an additional diffuse component must be added to the simulated images. This simulates various PSPC background components – particle, scattered solar, truly diffuse CXB, etc. The required diffuse component was determined through an iterative procedure as follows: (0) generate a "diffuse map" which is initially set to zero; (1) simulate sources as described in the previous paragraph; (2) add the Poisson-scattered "diffuse map"; (3) detect point sources and calculate the background map for the simulated image; (4) add the difference between

the background maps of the simulated and real images to the "diffuse map"; repeat steps (1)-(4) until the difference between the background maps of the simulated and real images is negligible.

Each ROSAT observation was simulated 5 times. The simulated data were formatted identically to the actual observations and processed in exactly the same manner as the real data. Several tests were used to check the quality of the simulated data. First, the log N - log S distribution determined from simulations was found to be in good agreement with the input one. Next, we checked that we do detect the same number of sources in the simulated and real data (both for the whole data set and for various subsets like short/long exposure, on-axis/off-axis etc.). In each case we found good agreement between the real data and simulations; for example, the total number of sources in the real data is 2158, while the number of sources averaged over the simulations is 2199 (which is less than 1σ difference).

The ACF was calculated as $\hat{w}(\theta) = \frac{DD}{RR} - 1$. Error bars for the ACF were determined assuming Poisson statistics (Peebles 1980). The resulting ACF is shown in Fig. 1. In the angular separation range of $25''$–$100''$ there is an $\sim 4\sigma$ detection (238 pairs found in the real data, 182 pairs are expected from simulations), and an $\sim 3.5\sigma$ detection between $100''$ and $500''$ (4513 pairs in the real data and 4276 in simulations). The power law model $w(\theta) = (\theta/\theta_0)^{1-\gamma}$ yields best fit parameters $\gamma = 1.7 \pm 0.3$ and a correlation angle $\theta_0 = 10'' \pm 8''$ (one-parameter 68% confidence intervals); if the value of γ is fixed at 1.8 (the value found for normal galaxies and optically selected quasars), the error in θ_0 is much smaller: $\theta_0 = 10'' \pm 2''$.

What is the origin of the positive correlation which we detect? Potential contributors to the small-scale correlation include extended sources like clusters of galaxies, nearby groups or even single galaxies of large angular size because they can be detected as multiple point sources. However, we have compiled the sample so that it does not contain such objects as targets of observations. In addition, we have searched through NED and SIMBAD and found that very few catalogued clusters, groups or nearby galaxies are contained in the inner field of view for the observations we used. Visual inspection of close pairs has shown that in only a few cases are the sources likely to be related to a single extended source; they are not "special" objects such as weak "sources" in the wings of the PSF around very bright sources or ghost images. Also, the detection of correlation at large separations ($100''$–$500''$) does not support the hypothesis that the correlation is due to the presence of a number of extended sources. Finally, the (relatively well-constrained) power law slope of the ACF is fully consistent with the power law slope of 1.8 found for normal galaxies (e.g. Davis & Peebles 1983) and the suggested value for optically selected quasars (Shanks & Boyle 1994). Thus it is likely that the observed correlation arises from clustering of QSOs, the most numerous class of faint X-ray sources (Boyle et al. 1993). Below we argue that the amplitude of the angular correlation

expected from the spatial correlation of optically selected quasars is in good agreement with our measurements, when the latter are appropriately corrected for the amplification bias which arises from the limited PSPC spatial resolution.

3. CORRECTION FOR THE AMPLIFICATION BIAS

Unfortunately, the best fit correlation angle $\theta_0 = 10''$ obtained for the directly measured ACF of the detected sources is smaller than the FWHM of the ROSAT PSPC PSF, which is $\sim 25''$ on-axis. This implies that sources separated by less than $\sim 20''$ are detected as a single object. Thus the distribution of detected sources is quite different from the distribution of real sources on the sky. It is clear that the spatial distribution of detected sources is close to the distribution of peaks in the pattern obtained by convolution of the distribution of real sources with the PSPC PSF. This is the origin of the amplification bias, which results in a more clustered distribution of peaks compared to the distribution of underlying objects. This effect was studied by Kaiser (1984) as applied to the correlation function of clusters of galaxies. Kaiser has shown that if one smoothes the galaxy distribution with a Gaussian window of ~ 10 Mpc size, the correlation function of peaks ("clusters") is biased with respect to the correlation function of galaxies: $\xi_{\rm clusters}(r) = A\xi_{\rm galaxies}(r)$. For reasonable values of model parameters, the amplification factor A can be as large as ~ 10. Therefore, we can expect that our results may be strongly affected by the amplification bias.

To determine the influence of the amplification bias, we have repeated the Monte-Carlo simulations described in section 2, with correlated input source positions. The sources with a power-law angular correlation function were simulated using the 2-dimensional version of the algorithm, described in Soneira & Peebles (1978). We fixed the power law slope of the input correlation function and adjusted its amplitude so that the ACF of detected sources (measured as described in section 2) is equal to that in the real data. For the simulations, we know the positions of both input and detected sources, so that we can determine the influence of the amplification bias. The ACFs of input and detected sources are shown in Fig 2. The power law shape of the input ACF was unaffected by the PSF and the detection algorithm, while the amplitude of the correlation function of detected sources is increased by a factor of 2.85. To check that the difference is indeed caused by the amplification bias, and not by an error in our detection algorithm, we also measured the ACF of peaks in the pattern obtained by the convolution of input source positions with the PSF. This is shown by open circles in Fig 2. The agreement of the ACF for detected sources and peaks is excellent. The success of this test makes us confident that we are indeed dealing with the amplification bias. The correction factor of 2.85 must be applied to the measured ACF in order to obtain

the unbiased estimate. With this correction, the correlation angle for the underlying source population is $\theta_0 = 4''$. In the following section we compare this corrected ACF with that expected for the sources clustered like optically selected quasars.

4. COMPARISON WITH OPTICAL AND OTHER X-RAY STUDIES

Most studies of QSO clustering show that quasars are indeed strongly clustered at $z \sim 1-2$. Although the reports on clustering evolution are controversial, there is a general agreement about the clustering amplitude at these redshifts – at a comoving scale of $10h^{-1}$ Mpc the amplitude of the two-point correlation function is ~ 1 (see Shanks & Boyle 1994 for a recent analysis). In the calculations below, we make a common assumption that the spatial two-point correlation function at any redshift is given by

$$\xi(r,z) \;=\; (r/r_0)^{-\gamma}\,(1+z)^{-3-\varepsilon} \tag{1}$$

with the parameter ε describing clustering evolution, for example $\varepsilon \simeq 3-\gamma \simeq -1.2$ corresponds to the clustering which is constant in comoving coordinates. For a power law spatial correlation function, the angular correlation function is also a power law $w(\theta) = (\theta/\theta_0)^{1-\gamma}$ with amplitude (Peebles 1980)

$$\theta_0^{1-\gamma} \;=\; r_0^{-\gamma}\,H_\gamma\,\left(\frac{H_0}{c}\right)^{\gamma}\,\frac{\int_0^\infty y^{5-\gamma}\,dy\,\phi(y)^2\,(1+z(y))^{-3-\varepsilon+\gamma}/F(y)}{[\int_0^\infty y^2\,dy\,\phi(y)/F(y)]^2}, \tag{2}$$

where $H_\gamma = \Gamma(\frac{1}{2})\,\Gamma(\frac{\gamma-1}{2})/\,\Gamma(\frac{\gamma}{2})$, and $F(y) = [1-\left(\frac{H_0 a_0 x}{c}\right)^2(\Omega-1)]^{1/2}$. The parameter y is related to the coordinate distance and redshift through

$$y \;=\; H_0 a_0\,\frac{x}{c} \;=\; 2\,\frac{(\Omega-2)(1+\Omega z)^{1/2}+2-\Omega+\Omega z}{\Omega^2(1+z)}, \tag{3}$$

and $\phi(y)$ determines the fraction of sources observable at the given y (or z), i.e. those with observed fluxes greater than the detection threshold $S_{\rm min}$. The cosmological model enters through the z – y relation (eq. 3), volume factor $F(y)$, and the selection function $\phi(y)$. The latter also depends on the source luminosity function evolution. Boyle et al. (1993) derive the cosmological evolution of QSOs in the form of pure luminosity evolution, with the characteristic luminosity scaling with redshift as $(1+z)^\beta$. For an object with luminosity $L(E)$ at redshift z, the observed energy flux is $f = L(E(1+z))(1+z)/4\pi D_L^2$, where D_L is the luminosity distance. For the power law energy spectrum $E^{-\alpha}$ with $\alpha = 1$ (which is close to what is observed, see Paper III), $L(E(1+z))(1+z) = L(E)$ so that the minimum luminosity is related to the minimum detectable flux simply as $L_{\rm min} = 4\pi\,D_L^2\,f_{\rm min}$. The

selection function can be written as

$$\phi(y) \;=\; \int_{L_{\rm min}}^{\infty} \Phi(L, z(y))\, dL \;=\; \int_{4\pi\, D_L^2 f_{\rm min}/R(z)}^{\infty} \Phi(L, 0)\, dL, \qquad (4)$$

where $\Phi(L, z)$ is the QSO luminosity function at redshift z, and $R(z)$ is the ratio of the typical luminosity at a redshift z to that at the present epoch. Given the spatial correlation function (eq. 1), the present day QSO luminosity function $\Phi(L, 0)$ and the evolution rate $R(z)$, eqns. 2-4 enable one to calculate the angular correlation amplitude, θ_0. Of numerous parameters in eqns. 1-4, the angular correlation function most strongly depends on the spatial clustering scale r_0, the rate of clustering evolution ε, and the power law slope γ. There is an indication that the value of γ is almost "universal", i.e. clustering of different classes of objects like galaxies, galaxy groups, clusters of galaxies, QSOs, is well described by a power law with indices close to 1.8, while the clustering scales r_0 are very different (see Bahcall 1988 for a review). As we showed aboved, $\gamma = 1.8$ is also in good agreement with the angular correlation of X-ray sources we report in this *Letter*. We hence fix γ at the value of 1.8 and calculate the angular correlation function for different values of r_0 and ε. We then compare the predicted and measured ACF, to constrain the parameters of the spatial correlation function. We assume that $\Omega = 1$ and the luminosity function and its evolution are those given by Boyle et al. (1993). The 90% confidence regions of parameters, calculated for two values of the QSO fraction,[2] are shown in Fig. 3. For simplicity of comparison of our results with the analysis of SH94, the clustering scale in Fig. 3 is expressed in units of the correlation length at $z = 1.5$. The grey-shaded region in this figure shows the range of clustering parameter values measured at $z = 1 - 1.5$ for optically selected quasars (Shanks & Boyle 1994). For any reasonable fraction of quasars in our X-ray sample, $0.5 \leq f \leq 1.0$, the X-ray and optical data are in good agreement.

We also compare our results with other studies of the X-ray background fluctuations. The angular correlation function of the *unresolved* background in ROSAT Deep Survey fields has been measured by Georgantopoulos et al. (1993) and SH94 who detect a positive correlation on small angular scales ($< 3'$). At larger separations rather tight upper limits on the angular correlation are obtained, and the general consensus (e.g., Carrera & Barcons 1992, Danese et al. 1993, SH94) is that a population of sources which are clustered like

[2] If the fraction of clustered sources $f_0 < 1$, and other sources are randomly distributed, the ACF of the total sample equals the ACF of clustered sources times f_0^2; if there are two populations both clustered, but independent from each other, the ACF must be multiplied by a factor f^2, $f_0 < f < 1$. In our calculations we assume that QSOs are clustered, while other sources are not.

QSOs cannot produce more than $30\% - 50\%$ of the *still unresolved* XRB. For example, Fig. 8 of SH94 shows that the isotropy of the residual XRB requires that a population of sources which contribute 100% of the residual XRB must have a correlation length $x_0 \leq 2h^{-1}$ Mpc at $z = 1.5$. This is significantly below the correlation length of both QSOs and the X-ray sources in our sample. Thus, there is a considerable discrepancy: on the one hand, directly detected X-ray sources are highly correlated (their clustering is consistent with $\sim 80\%$ of them being spatially distributed like QSOs), while the residual XRB (after subtraction of detected sources) appears very smooth. This may imply significant changes in the nature of sources contributing to the XRB at faint flux levels (close to the sensitivity limit of ROSAT Deep surveys). Narrow emission line galaxies identified in Deep surveys (e,g., Boyle et al. 1995) may be promising candidates for a new population. Also, one cannot exclude a significant contribution of truly diffuse emission to the unresolved XRB. Hasinger et al. (1993b) showed that the contribution of a diffuse component up to 25% of the total XRB flux is not excluded. Wang & McCray (1993) found that 40% of the XRB in the $0.5 - 0.9$ keV band arises from a diffuse thermal component. Both results indicate that a significant fraction of the unresolved XRB may be truly diffuse, thus making it very smooth compared to the clustering found for detected sources.

We have made a rough estimate of the contribution of the observed point source correlation to that reported by SH94 for the unresolved XRB since we detect sources below their threshold (see Paper II). SH94 gave a 2σ limit of 30-35% for the fraction of unresolved sources contributing to the XRB that could be clustered like quasars based on analysis of images with a typical flux limit of about 1×10^{-14} ergs s^{-1} cm^{-2}. Above this threshold $\sim 40\%$ of the soft XRB is resolved into point sources. The sources in the flux range $1.5 - 10 \times 10^{-15}$ ergs s^{-1} cm^{-2} (i.e. between the typical sensitivities of the deepest field and SH94) comprise $\sim 30\%$ of the XRB. If these faint sources are clustered not significantly less than the majority of our sources (around a flux of 10^{-14} ergs s^{-1} cm^{-2}), a large fraction of the maximum correlation allowed by SH94's limit for the "residual" XRB must be accounted for by the sources we detect. If bright and faint sources exhibit the same clustering, SH94's 2σ upper limit for the correlation in the "unresolved" XRB is produced. In this case the XRB below 1.5×10^{-15} ergs s^{-1} cm^{-2}, which comprises $\sim 35\%$ of the total XRB, should exhibit essentially no clustering since we have already observed the quasar-like, clustered population allowed by the SH94 limit.

5. CONCLUSIONS

We report on the first detection of a positive angular correlation derived from the distribution of individual, faint X-ray sources. This correlation is detected with high statistical significance on both small ($\lesssim 1'$) and moderate ($1'$–$10'$) angular scales. The two-point angular correlation function is well described by a power law $(\theta/\theta_0)^{1-\gamma}$, with $\gamma = 1.7 \pm 0.3$ which is remarkably close to the corresponding value for normal galaxies and optically selected quasars. We show that the amplitude of correlation is also consistent with the hypothesis that X-ray sources are spatially distributed in the same way as optically selected quasars.

We thank S. Murray for his comments and continued interest and support of this project and we thank C. Jones for comments on the manuscript. We thank the referee, K. Jahoda, for helpful comments and a critical reading of the manuscript. This work was supported by NASA contract NAS8-39073. We acknowledge support from SUN Microsystems through a hardware grant. A.V. thanks CfA for its hospitality during his visit. A.V. was supported by the RBRF grant 95-02-05933.

REFERENCES

Bahcall, N.A. 1988, ARA&A, 26, 631.

Boyle B.J., Griffiths, R.E., Shanks, T., Steward G.C., & Georgantopoulos, I. 1993, MNRAS, 260, 49.

Boyle, B.J., McMahan, R.G., Wilkes, B.J., Elvis, M. 1995, MNRAS, 272, 462.

Carrera, F.J., & Barcons, X. 1992, MNRAS, 257, 507.

Danese, L., Toffolatti, L., Franceschini, A., Martin-Mirones, J.M., and De Zotti, G. 1993, ApJ, 412, 56.

Davis, M., & Peebles, P.J.E. 1983, ApJ, 267, 465.

Georgantopoulos, I., Stewart, G.C., Shanks, T., Griffiths, R.E., Boyle, B.J. 1993, MNRAS, 262, 619.

Hasinger, G., Boese, G., Predehl, P., Turner, T., Yusaf, R., George, I., & Rohrbach, G. 1993, GSFC OGIP Calibration Memo CAL/ROS/93-015.

Hasinger, G., Burg, R., Giacconi, R., Hartner, G., Schmidt, M., Trumper, J., and Zamorani, G. 1993b, å, 275, 1.

Kaiser, N. 1984, ApJ, 284, L9.

Peebles, P.J.E. 1980, The Large Scale Structure of the Universe (Princeton: Princeton University Press).

Shanks, T., & Boyle, B.J. 1994, MNRAS, 271, 753.

Snowden, S.L., McCammon, D.; Burrows, D.N., & Mendenhall, J.A. 1994, ApJ, 424, 714.

Soltan, A., & Hasinger, G. 1994, A&A, 288, 77 (SH94).

Soneira, R.M., & Peebles, P.J.E 1978, AJ, 83, 845.

Vikhlinin A., Forman, W., Jones, C., & Murray, S. 1995a, ApJ, 451, 564. (Paper I)

Vikhlinin A., Forman, W., Jones, C., & Murray, S. 1995b, ApJ, 451, 553. (Paper II)

Vikhlinin A., Forman, W., Jones, C., & Murray, S. 1995c, ApJ, 451, 542. (Paper III)

Wang, Q.D., & McCray, R. 1993, ApJ, 409, L37.

Figure Captions

Fig. 1.—Angular two-point correlation function of X-ray sources. The best fit power law model $(\theta/\theta_0)^{1-\gamma}$ is shown by the dashed line. The power law slope is relatively well constrained and γ is remarkably close to that for normal galaxies and optically selected quasars (1.8).

Fig. 2.—Comparison of the simulated and measured ACF. The source positions were simulated so that the ACF of detected sources in simulations (open circles) is equal to that of sources detected in the real data (fit is shown by the solid line). The ACF of input positions is shown by small solid squares; the dashed line is the power law $\theta^{-0.8}$ fit to the input ACF. The shapes of the input and measured ACF are the same, while the latter has a factor of 3 higher normalization. To verify that the difference is due to the amplification bias, the input source positions were convolved with the PSPC PSF, and the ACF of peaks in the convolved pattern has been measured (large solid circles).

Fig. 3.—The 90% confidence intervals for the correlation length x_0 at $z = 1.5$ (in comoving coordinates) and the evolution parameter ε. Assuming 1) a spatial correlation function of the form $\xi(r, z) = (r/r_0)^{-\gamma}\ (1+z)^{-3-\varepsilon}$, 2) a source luminosity function and evolution that of X-ray selected quasars as given by Boyle et al. (1993), and 3) $\Omega = 1$, the angular correlation function was calculated for two values of the clustered population fraction $f = 0.6, 1.0$ and compared with the measured ACF (Fig. 1) by means of a χ^2-test. The grey-shaded region shows the range of values of x_0 measured for optically selected quasars (Shanks & Boyle 1994). X-ray and optical data are in good agreement if the QSO fraction is 60%-80%, close to what is observed.

Fig. 1

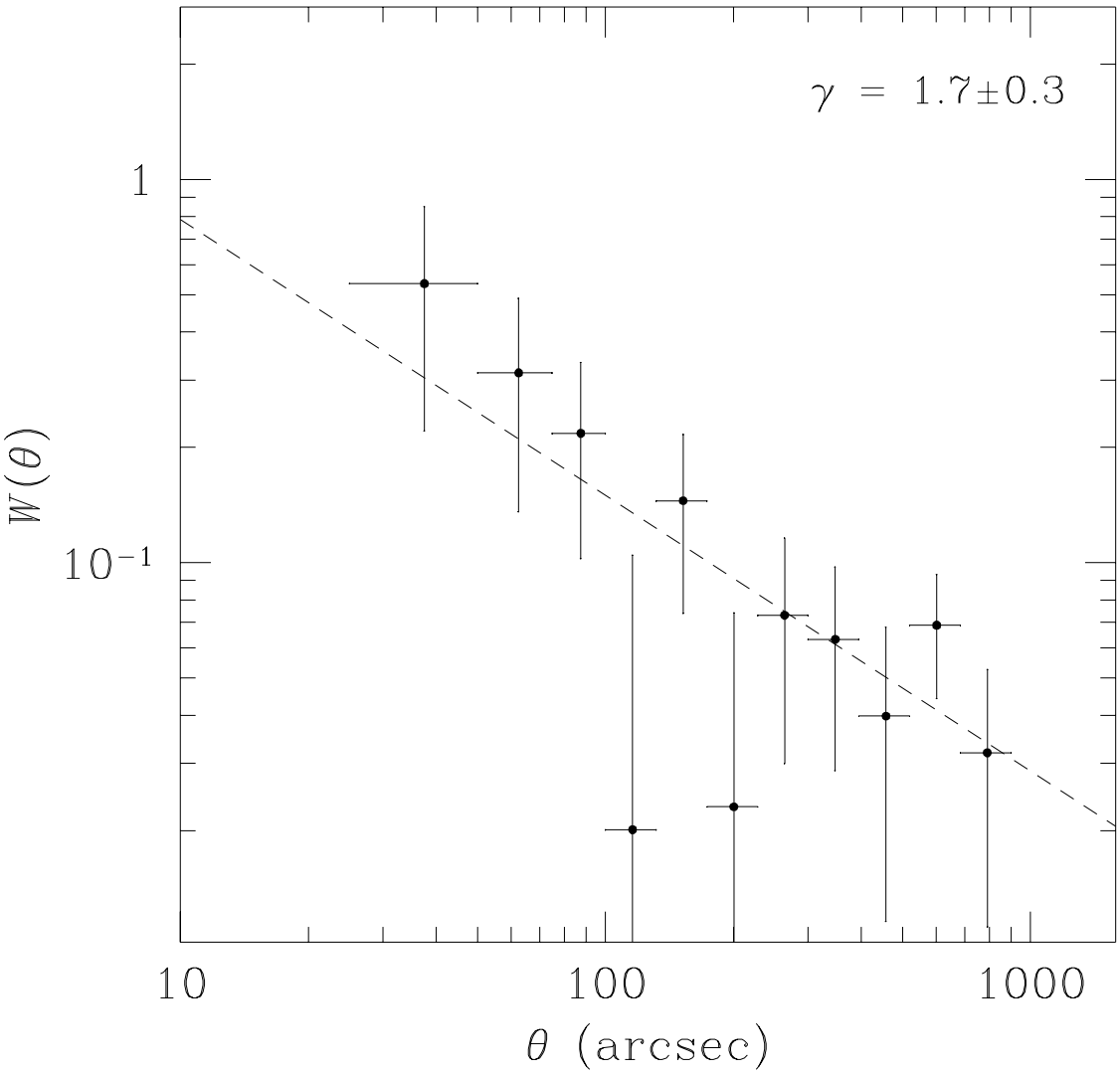

Fig. 2

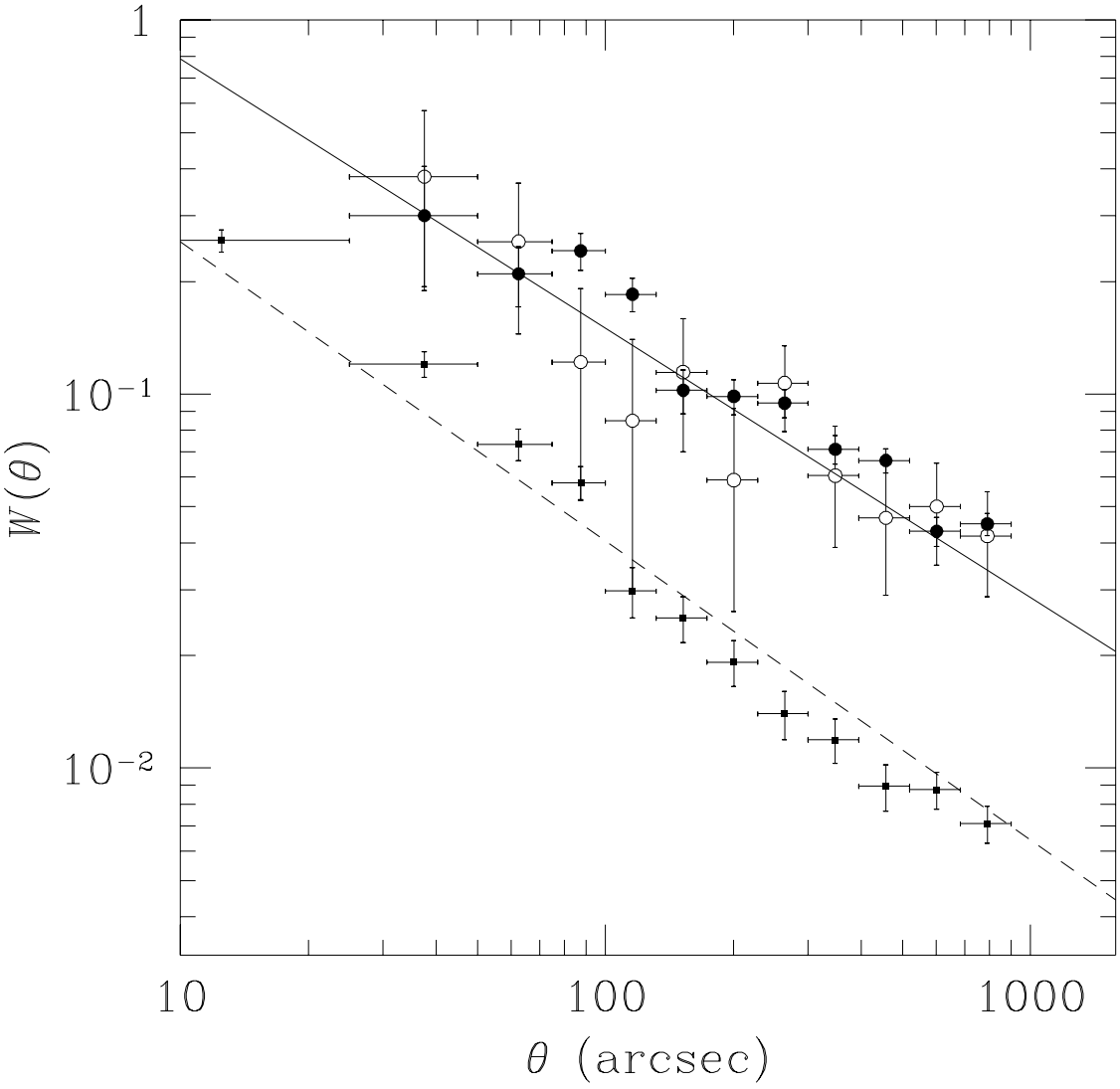

Fig. 3